Comparison of the ultrafast to slow time scale dynamics of three liquid crystals in the isotropic phase

S. D. Gottke and Hu Cang
Department of Chemistry, Stanford University, Stanford, California 94305

Biman Bagchi
Solid State and Structural Chemistry Unit, Indian Institute of Science, Bangalore 560 012, India

M. D. Fayer
Department of Chemistry, Stanford University, Stanford, California 94305

(Received 24 December 2001; accepted 25 January 2002)

The dynamics of three liquid crystals, 4′(pentyloxy)-4-biphenylcarbonitrile (5-OCB), 4′-pentyl-4-biphenylcarbonitrile (5-CB), and 1-isothiocyanato-(4-propylcyclohexyl)benzene (3-CHBT), are investigated from very short time (~1 ps) to very long time (>100 ns) as a function of temperature using optical heterodyne detected optical Kerr effect experiments. For all three liquid crystals, the data decay exponentially only on the longest time scale (> several ns). The temperature dependence of the long time scale exponential decays is described well by the Landau–de Gennes theory of the randomization of pseudonematic domains that exist in the isotropic phase of liquid crystals near the isotropic to nematic phase transition. At short time, all three liquid crystals display power law decays. Over the full range of times, the data for all three liquid crystals are fit with a model function that contains a short time power law. The power law exponents for the three liquid crystals range between 0.63 and 0.76, and the power law exponents are temperature independent over a wide range of temperatures. Integration of the fitting function gives the empirical polarizability–polarizability (orientational) correlation function. A preliminary theoretical treatment of collective motions yields a correlation function that indicates that the data can decay as a power law at short times. The power law component of the decay reflects intradomain dynamics. © *2002 American Institute of Physics.* [DOI: 10.1063/1.1462039]

I. INTRODUCTION

The orientational relaxation dynamics of liquid crystals in the isotropic phase differ from those of conventional liquids. Relatively close to the nematic–isotropic ($N-I$) phase transition, orientational relaxation dynamics are strongly influenced by local structures (pseudonematic domains) that exist in the isotropic phase.[1,2] A great deal of experimental work has been done, using both time and frequency domain methods, to examine the relatively long time scale orientational relaxation that is dominated by the randomization of the pseudonematic domains.[3–11] Near the $N-I$ phase transition, the isotropic phase is nematically ordered on a distance scale defined by a correlation length, ξ.[1,2] As the $N-I$ phase transition is approached from above, ξ grows, becoming infinite in the nematic phase. On time scales of many nanoseconds to hundreds of nanoseconds, depending on the temperature, the local order randomizes, giving rise to exponential decays of time domain optical Kerr effect experiments.[3,11]

The long time scale relaxation of the local structures is described by Landau–de Gennes (LdG) theory, which was formulated a number of years ago to account for effects on dynamics of the $N-I$ phase transition and nematic-like order above the phase transition.[1] The $N-I$ phase transition is weakly first order, and it has a noticeable effect on properties of the liquid near the phase transition temperature, T_{NI}. LdG theory predicts the temperature dependence of long time exponential decay in the isotropic phase, which has a sharply increasing decay time as the transition temperature is approached. LdG theory has been confirmed many times experimentally using techniques such as optical Kerr effect,[3,4,11] depolarized light scattering,[5] dynamic light scattering,[6] magnetic, [7] and electric birefringence,[8] and dielectric relaxation.[9,10] The influence of the pseudonematic domains on the long time scale dynamics continues up to ~50 K above the $N-I$ phase transition temperature.[11] LdG theory gives the correlation length as

$$\xi(T)=\xi_0[T^*/(T-T^*)]^{1/2}, \tag{1}$$

where ξ_0 is the molecular length scale (typically 7–8 Å), and T^* is a temperature 0.5–1.0 K lower than T_{NI}.[2] (Properties scale as T^* is approached rather than T_{NI} because the phase transition has both first- and second-order character.) At high temperatures, the size of the domain becomes similar to the molecular volume, and LdG theory ceases to apply.

On time scales short compared to the time for pseudonematic domain randomization, and on distance scales short compared to ξ, nematogens exist in an environment with nematic like order. Dynamics on short time scales (less than a few ns) are not described by the LdG theory. The dynamics will be strongly influenced by the local order. A number of studies in the past decade have investigated orientational relaxation dynamics in the short time regime.[11–16] Previous transient grating optical Kerr effect experiments, which mea-

sure the time derivative of the polarizability-polarizability correlation function[17–20] (equivalent to the orientational correlation function, except on <1 ps time scales), revealed power law decays at short times and the LdG exponential decay at long times. The data were fit with a model function consisting of a power law (short time intradomain dynamics) plus an exponential (domain randomization). Theoretical treatments based on single particle dynamics produced power law functions,[21,22] but, as discussed below, do not describe the data appropriately. Because of limitations of signal to noise ratios on the data, the initial experiments did not measure the full time dependence, from very short times to very long times, as a single continuous curve. The data were analyzed piecewise.

Recently, improvements in experimental technique have made it possible to examine the full time dependence as a function of temperature. The liquid crystal 1-isothiocyanato-(4-propylcyclohexyl)benzene (3-CHBT) was studied in the isotropic phase using optical heterodyne-detected optical Kerr effect (OHD-OKE) experiments.[23] The data were fit with a more complicated function than the sum of a power law and an exponential. The fitting function was able to describe the full time dependence. The results showed that a power law, with a temperature independent exponent, dominates the short time scale behavior. The temperature independent power law decay is followed by an exponential decay on a relatively short time that then goes over to the long time scale LdG exponential decay. Integration of the analytical fitting function provides a model of the polarizability–polarizability (orientational) correlation function.[23] This model correlation function does not contain a power law, but its derivative does. A preliminary theoretical analysis that calculates the orientational correlation function on fast time scales, based on a description of the collective orientational relaxation, was presented. The theoretical correlation function is not a power law, but its derivative displays a power law like decay at short time.[23]

In this paper, two additional liquid crystals, 4′-(pentyloxy)-4-biphenylcarbonitrile (5-OCB) and 4′-pentyl-4-biphenylcarbonitrile (5-CB), are studied, and the results are compared to those obtained on 3-CBHT.[23] Figure 1 displays the chemical structures of the three liquid crystals. The data for all three liquid crystals on all time scales ($\sim$1 ps to $>$100 ns) and over a wide range of temperatures can be fit exceedingly well by the same function. All three liquid crystals display LdG behavior on the longest time scale. The data for all three liquid crystals decay as power laws (t^{-p}) on the short time scale. All three power law exponents are temperature independent over the full range of temperatures studied. The power law exponents are similar for the three liquid crystals, with p equal to 0.63 (5-OCB), 0.65 (5-CB), and 0.76 (3-CHBT). The facts that all three liquid crystals can be fit exceeding well by the same fitting function, that all three liquid crystals have temperature independent power law decays in the OHD-OKE experiments, and that all three liquid crystals obey LdG theory at long time indicate that the isotropic phase of liquid crystals have a universal behavior on all time scales. The short time scale power law decays (derivative of the correlation function) are examined in the context of the recently presented theory, which was derived on the basis of collective orientational relaxation of the nematogens.

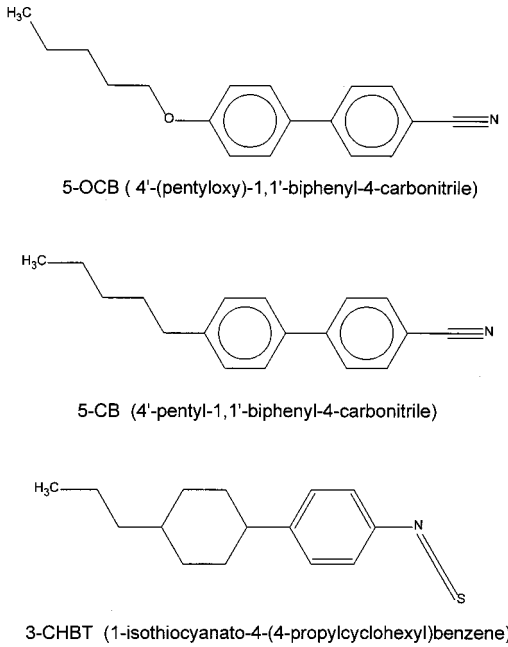

FIG. 1. The chemical structures of the three nematogens, 5-OCB, 5-CB, and 3-CHBT.

II. EXPERIMENTAL PROCEDURES

Optical heterodyne-detected optical Kerr effect (OHD-OKE) spectroscopy[24] was used to measure the liquid crystal orientational relaxation. A pump pulse creates a time-dependent optical anisotropy that is monitored via a heterodyne detected probe pulse with a variable time delay. The OHD-OKE experiment measures the system's impulse response function, which is the time derivative of the polarizability–polarizability (orientational) correlation function. The methods for the analysis of OHD-OKE data have been described in detail.[25] The Fourier transform of the OHD-OKE signal is directly related to data obtained from depolarized light scattering,[26] but the time domain OHD-OKE experiment can provide better signal to noise ratios over a broader range of times for experiments conducted on very fast to moderate time scales.

To observe the full range of liquid dynamics, at each temperature several sets of experiments were performed with different pulse lengths and delays. For times $t<30$ ns, a mode-locked 5 kHz Ti:sapphire laser/regenerative amplifier systems was used ($\lambda=800$ nm for both pump and probe). The pulse length was adjusted from 75 fs to 100 ps to improve S/N. The shortest pulses were used for times 100 fs to a few tens of ps. For longer times, a few ps to 600 ps, the pulses were lengthened to 1 ps. The longer pulses produce more signal for the longer time portions of the data. For intermediate times, the pulse compression was bypassed, and a 100 ps pulse was used with a long delay line to obtain data from 100 ps to 30 ns. Because the experiments are nonresonant optical Kerr effect measurements, a frequency chirp on

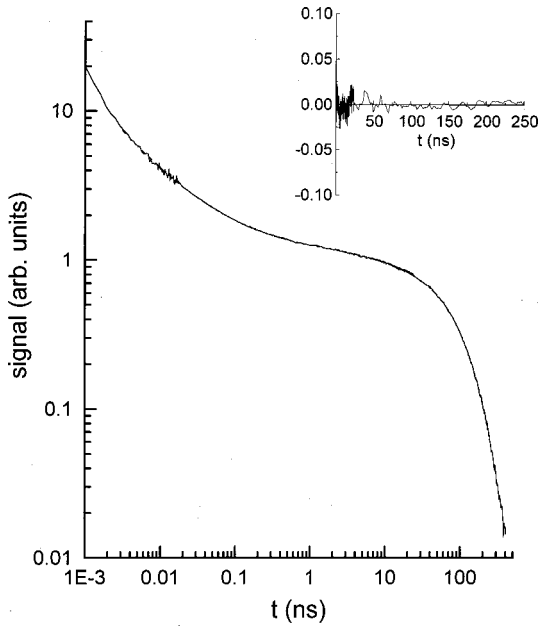

FIG. 2. Optical heterodyne detected optical Kerr effect data displaying the time dependence of orientational dynamics of the liquid crystal, 5-OCB at 347 K on a log plot. The data span the time range 1 ps to 400 ns. At short time, the data decay as a power law. At long time, the data decay exponentially. Also shown is a fit to the data using Eq. (2). The fit is very good over the broad time range. The residuals of the fit are shown in the inset.

the pulse does not influence the data. For even longer times, a CW diode laser was used for probing, and a fast digitizer (2 ns per point) recorded the data. The scans taken over various time ranges always overlapped substantially permitting the data sets to be merged by adjusting only their relative amplitudes. Additional experimental details have been published recently.[27]

5-OCB, 5-CB, and 3-CHBT were purchased from Aldrich and used without further purification except for filtration through a 0.2 μm disk filter to reduce scattered light. The samples were sealed under vacuum in 1 cm glass cuvettes. The cuvettes were held in a constant flow cryostat where the temperature was controlled to ± 0.1 K. Experiments were performed in the isotropic phase from 344 to 385 K for 5-OCB, 311 to 346 K for 5-CB, and 315 to 355 K for 3-CHBT.

III. RESULTS AND DISCUSSION

Figure 2 displays a typical data set for 5-OCB at 347 K ($T_{NI}=344$ K). The data, which are plotted on a log–log scale, span the range of times from 1 ps to 400 ns. Starting at short times, the data falls steeply; the decay becomes more gradual at intermediate times on the log plot, and it finally falls very steeply at long time. The long time scale data (>15 ns) is a single exponential as expected from LdG theory. Also shown on the plot is a fit to the data and the residuals of the fit using the function discussed below. The fit follows the data so well that it is barely discernable on the plot. All of the fits to the data sets at various temperatures for the three liquid crystals display essentially the same quality of fit.

The data can be divided into two time regimes, that is, the LdG relaxation time scale and times fast compared to the LdG relaxation time, τ_{LdG}. The qualitative explanation for the two time regimes has been discussed previously.[12] The following is a brief explanation. In the isotropic phase, the macroscopic liquid has an order parameter, $S=0$, that is, macroscopically there is no orientational order. However, on a distance scale short compared to ξ, and on a time scale short compared to τ_{LdG}, there is pseudonematic order, which can be characterized by a local order parameter, S_L, relative to a local director. When the pump pulse *E*-field is applied, the nematogens experience a torque that produces a slight alignment with the field. When the field is removed, the macroscopic system is left with $S\neq 0$. Field free evolution will reestablish $S=0$.

To understand the origin of the dynamical time scales, it is necessary to consider the problem microscopically. There are two contributions to the relaxation, intradomain relaxation and domain randomization (LdG relaxation). The *E*-field induces a small net alignment of the individual molecules. The molecular alignments change the local order parameter, S_L. Unlike *S*, which is a macroscopic parameter, S_L, is nonzero prior to the application of the optical field. S_L defines the local nematic structure relative to the local director associated with a given pseudo-nematic domain. Initially, $S_L=S_L^0$. Immediately following the application of the field, $S_L>S_L^0$. (S_L can also be $<S_L^0$, depending on the direction of the local director relative to the field direction.) The small alignment of the molecules with the field changes S_L, and it also rotates the direction of the local director. Fast intradomain relaxation occurs, restoring the local order parameter to S_L^0. Relaxation of the perturbed local order back to S_L^0 occurs on the fast time scales but leaves the ensemble of domain local directors still slightly aligned with the direction defined by the *E*-field.[12] This long-lived anisotropy can only decay by randomization of the domains and is responsible for the long time decay described by LdG theory.

In Fig. 2, the fit to the data and the calculation of the residuals used the model function,[23]

$$f(t)=e^{-t/\tau_{\mathrm{LdG}}}\left[a+e^{-t/\gamma}\left(b+\left(\frac{t}{t_\delta}\right)^{-p}\right)\right]. \tag{2}$$

Here, τ_{LdG} is the decay constant of the LdG single exponential decay with an amplitude of *a*. All other terms apply to the intradomain relaxation. The exponential term contained inside the square brackets with a decay constant of γ is the intermediate exponential decay that flattens out the curve. The power law term with an exponent of $-p$ is scaled by t_δ. All of the terms inside the square brackets describe the intradomain, non-LdG, decay. The intradomain decay leaves a residual anisotropy of amplitude *a*, which then decays via the domain randomization with τ_{LdG}. The fit to the 5-OCB at 347 K data shown in Fig. 2 uses the parameters, $\tau_{\mathrm{LdG}}=88.3$ ns, $\gamma=12.5$ ns, $p=0.62$, $a=1.01$, $b=0.12$, $t_\delta=0.059$ ns. The function in Eq. (2) does an excellent job of describing the data over a wide range of times. The inset shows the residuals of the fit to the data. The function given in Eq. (2) works at all temperatures, and it describes the data equally well for three different liquid crystals. While there are a large number of parameters in Eq. (2), they can be determined quite accurately because some of them are rela-

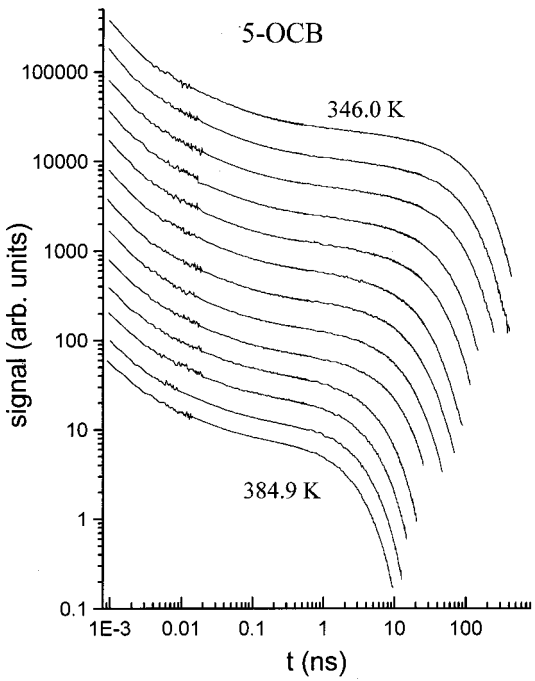

FIG. 3. Temperature dependent 5-OCB data sets displayed on a log plot. The data sets have been offset for clarity of presentation. Starting with the top most curve, the temperatures for the data sets are 346.0, 347.0, 348.0, 350.1, 352.1, 355.0, 357.0, 360.0, 363.0, 370.0, 374.9, 380.0, 384.9 K.

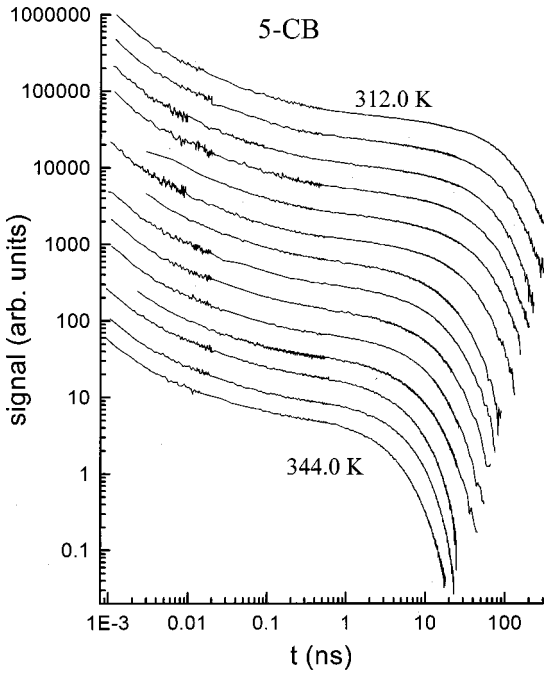

FIG. 4. Temperature dependent 5-CB data sets displayed on a log plot. The data sets have been offset for clarity of presentation. Starting with the top-most curve, the temperatures for the data sets are 312.0, 312.9, 314.0, 315.0, 316.0, 318.0, 322.0, 324.0, 326.0, 329.0, 332.0, 336.0, 339.0, 344.0 K.

tively independent of the others. The long time portion of the data is a single exponential, which makes it possible to determine τ_{LdG} independently of the other parameters. The short time behavior is dominated by the power law, which makes it possible to determine p and t_δ. The intermediate time scale exponential is the most difficult to determine accurately because it is sandwiched between the short time scale power law and the long time scale LdG exponential decay. The data cannot be fit without the intermediate term, but the decay constant has larger error bars than those associated with the other parameters (see below).

The previous function used to describe the data, the simple sum of a power law and an exponential,[12,13,21] does not accurately reproduce the intermediate time scale data (just prior to the LdG decay) nor does it properly describe the very long time behavior. It also contains a fundamental conceptual flaw. At sufficiently high temperature, the LdG decay becomes very fast. At even higher temperature, domains cease to exist, and the decay should become a single fast exponential. With a functional form that is the sum of a power law and an exponential (the function used in prior work[12,13,21]), making the exponential very fast leaves a long time decay that is a power law. This is contrary to observation. Even for the decays at moderate temperature, at sufficiently long time, the simple sum of a power law and an exponential leaves a long power law tail. The present data are good enough and go out far enough in time that comparison to the simple sum shows deviations from the data at long time as well as at intermediate times. The function in Eq. (2) does not have these problems. The intradomain terms decay, leaving a residual anisotropy that decays exponentially. If the LdG decay becomes very fast, then the entire function decays exponentially.

At higher temperatures ($>$357 K for 5-OCB, $>$329 K for 5-CB, and $>$325 K for 3-CHBT), τ_{LdG} is the same magnitude or shorter than the intermediate time constant γ, and it becomes very difficult to distinguish the two time constants. The difficulty in distinguishing the two terms is compounded by the fact that the amplitude, a, associated with the LdG term in Eq. (2) is generally five to six times larger than b, the amplitude associated with the intermediate exponential. In Eq. (2), multiplying through by the outer exponential, $\exp(-t/\tau_{\mathrm{LdG}})$, causes the inner exponential to have the decay constant,

$$K=\frac{1}{\tau_{\mathrm{LdG}}}+\frac{1}{\gamma}.$$

At the higher temperatures, effectively $K=1/\tau_{\mathrm{LdG}}$.

Figure 3 shows the full temperature dependent data sets for 5-OCB plotted on a log plot and offset vertically for clarity. The lowest temperature is at the top. The temperature for each curve is given in the figure caption. Figure 4 is the same type of graph for 5-CB, and Fig. 5 is for 3-CHBT. For all three liquids, the qualitative trends are exactly the same. Fast time decays look very similar to one another, while the long exponential decay changes rapidly with temperature.

The LdG exponential time constant is expected to have a temperature and viscosity dependence given by[1–3,11]

$$\tau_{\mathrm{LdG}}=\frac{V^*_{\mathrm{eff}}\eta(T)}{k_B(T-T^*)^\gamma}, \tag{3}$$

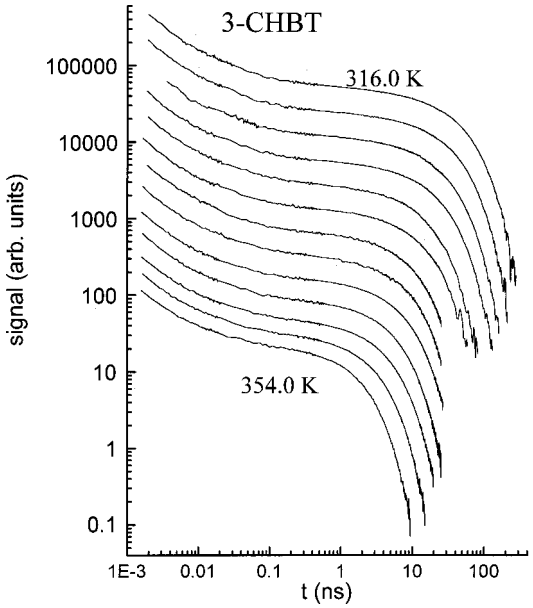

FIG. 5. Temperature dependent 3-CHBT data sets (Ref. 23) displayed on a log plot. The data sets have been offset for clarity of presentation. Starting with the topmost curve, the temperatures for the data sets are 316.0, 317.0, 318.0, 319.1, 321.5, 323.0, 325.1, 327.0, 319.0, 333.1, 337.0, 344.0, 354.0 K.

where V^*_{eff} is the approximate molecular volume, η is the viscosity, k_B is the Boltzmann constant, T^* is defined above, and $\gamma=1$ according to mean field theory and is observed to be 1.[11] Figure 6 displays the long time exponential decay

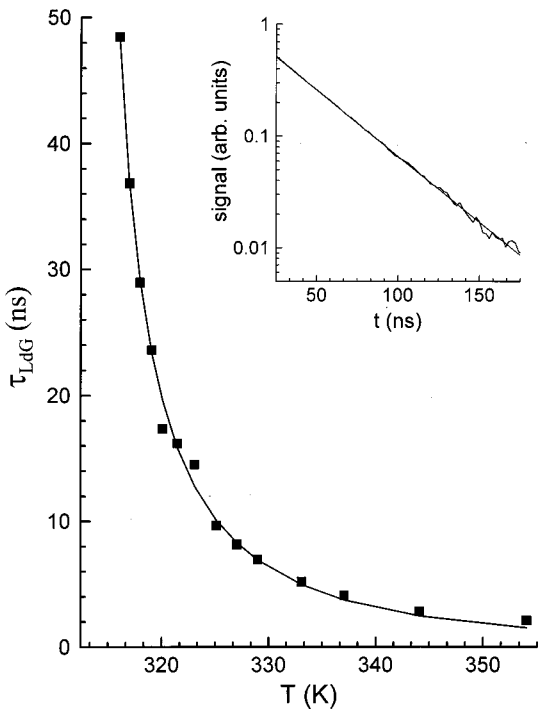

FIG. 6. The 3-CHBT long time scale exponential decay time as a function of temperature. The temperature dependence of the decay time is predicted by the Landau–de Gennes theory. The solid curve through the data is the theoretically predicted LdG curve. The inset shows the long time portion of the 317 K data set on a semilog plot with a line through the data showing the decay is exponential.

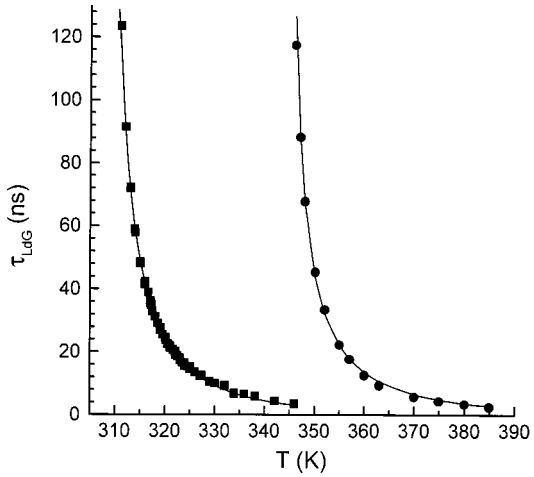

FIG. 7. The temperature dependence of the decay times (τ_{LdG}) of long time exponential portions of the data for 5-CB (squares) and for 5-OCB (circles). The solid curves through the data are the theoretically predicted LdG curves.

times, τ_{LdG}, as a function of temperature for 3-CHBT. The inset displays the long time portion of the data at 317 K on a semilog plot. A line is shown passing through the data. As can be seen in the inset, the long time portion of the data is described very well as an exponential decay. This is true of the long time data at all temperatures for the all three liquid crystals. Using Eq. (2) to fit the data or fitting only the long time tail to an exponential gives identical results for τ_{LdG}. The curve through the data in Fig. 6 is obtained from Eq. (2) using V^*_{eff} as a scaling parameter. V^*_{eff} does not change the shape of the curve; it only sets the magnitude. T^* was found to be 312.5 K. Clearly, the long time behavior of 3-CHBT is described very well by LdG theory, as is expected. Figure 7 displays the temperature dependence of the decay time (τ_{LdG}) of long time exponential portions of the data for 5-CB (squares) and for 5-OCB (circles). Again, V^*_{eff} was varied as a scaling parameter. T^* was found to be 307.2 K for 5-CB and 343.5 K for 5-OCB. These are in accord with the T_{NI} values for each liquid. Like the 3-CHBT data (Fig. 6), the LdG theory describes the temperature dependence of the long time exponential portions of the data very well.

Figure 8 shows a 5-OCB dataset at 317 K with both exponential terms of Eq. (2) subtracted from the data. The resulting power law has an exponent of $p=0.63$, and can be seen over almost three decades. When the same procedure is applied to the 5-CB and 3-CHBT (Ref. 23) data, similar long power law decays become evident. In Fig. 9, values are plotted for the power law exponent [Fig. 9(a)], and for the intermediate exponential time constant [Fig. 9(b)] for 5-OCB (squares), 5-CB (circles), and 3-CHBT (triangles). The power law exponents, p, for all three liquids are constant, within experimental uncertainty, over the full temperature ranges studied. The p values are 0.63 ± 0.01 (5-OCB), 0.65 ± 0.01 (5-CB), and 0.76 ± 0.03 (3-CHBT).

The intermediate exponential decay constant γ [Fig. 9(b)] has much greater uncertainty in the values at each temperature than the power law exponent of the τ_{LdG} decay constant. The uncertainty in the γ values is produced by the

relatively small magnitude of the intermediate decay component and its position between the power law and the LdG decay. While there may appear to be a weak temperature dependence, the relatively large variations in the values from one temperature to another suggests that apparent temperature dependence probably arises from experimental error. Treating the γ values as temperature independent, the γ values are 12.6 ± 2.1 (5-OCB), 11.8 ± 2.4 (5-CB), and 7.8 ± 3.0 (3-CHBT).

The model function for the decay given in Eq. (2) describes the data well. This function is related to the time derivative of the polarizability-polarizability correlation function. By integrating Eq. (2) and normalizing the function at $t=0$, an empirical correlation function is obtained, that is,

$$C(t)=\frac{a\tau_{\mathrm{LdG}}e^{-t/\tau_{\mathrm{LdG}}}+(b/K)e^{-Kt}+(1/t_\delta)^{-p}K^{p-1}\Gamma(1-p,Kt)}{a\tau_{\mathrm{LdG}}+(b/K)+(1/t_\delta)^{-p}K^{p-1}\Gamma(1-p)}, \tag{4}$$

where K is defined above, and $\Gamma(x)$ is the gamma function, and $\Gamma(x,y)$ is one of the definitions of the incomplete gamma function,[28]

$$\Gamma(x,y)=\int_y^\infty e^{-s}s^{x-1}ds.$$

All of the parameters in the expression for the power law are obtained from the fits to the experimental data. While the correlation function given in Eq. (4) is empirical, a correlation function derived theoretically from first principles will display the same time dependent behavior. Therefore, Eq. (4) is useful for comparison to theoretical calculations of the full correlation function.

Previous theoretical examination of the short time behavior treated the problem calculating a single particle correlation function.[21,22] These calculations did yield power laws. However, the correlation functions were compared directly to the data; the required derivative was not taken. Once the derivative is taken, the calculated decays are much steeper than the data, that is, the power law exponent in the derivative function is too large. More important, the single particle correlation function should only apply at extremely short time. The time scales observed in the experiments reflect the collective dynamics of the local nematically ordered structures. An initial theory of the collective correlation function at short times, the derivative of which decays approximately as a power law on the fast time scale, has recently been presented.[23]

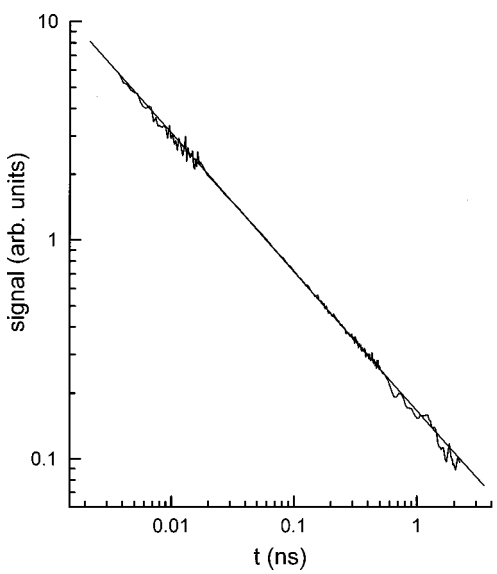

FIG. 8. The short time portion of the 5-OCB data at 347 K with the exponential contributions removed [see Eq. (2)] on a log plot. The line through the data shows that the decay is a power law from 3 ps to 2 ns.

As the function measured in optical Kerr experiments is the time derivative of the *total* polarizability–polarizability time correlation function, the response is determined primarily by the time correlation function of the second rank spherical harmonics.[29] In Kerr experiments, we measure the collective, that is, the $k=0$ limit of $C_{2m}(k,t)$. In its current form, the theory calculates the $C_{20}(k,t)$ correlation function. The correlation function is calculated in the Laplace frequency plane, that is, $C_{20}(k,z)$, using a general molecular hydrodynamic approach.[30–32] After a rather lengthy derivation, and inversion of the final expression into the time domain, the short time expression for the polarizability–polarizability correlation function is[23]

$$C_{20}(t)=\exp(a^2t)\,\mathrm{erfc}(at^{1/2}), \tag{5a}$$

where erfc is complementary error function.[28] The parameter a is given by[23]

$$a=\rho B^3(6D_R)^{1/2}f_{220}(k=0)/3. \tag{5b}$$

ρ is the number density, and D_R is the rotational diffusion coefficient of the nematogens. $f_{220}(k)$ is the dimensionless orientational caging parameter defined by

$$f_{220}(k)=1-(\rho/4\pi)c_{220}(k), \tag{5c}$$

where $c_{220}(k)$ is the (220) component of wave vector and orientation dependent direct correlation function. B is related to the second derivative of the direct correlation function $c_{220}(k)$ at $k=0$, that is,

$$B^2=\frac{\rho}{4\pi}\left(\frac{d^2c_{220}}{dk^2}\right)_{k=0}. \tag{5d}$$

Equation (5) for $C_{20}(t)$ is the main result of the theoretical analysis. It is expected to be valid in a time window that is short compared to τ_{LdG} but long compared to the ultrashort time scale of collisional dynamics. Equation (5) shows that

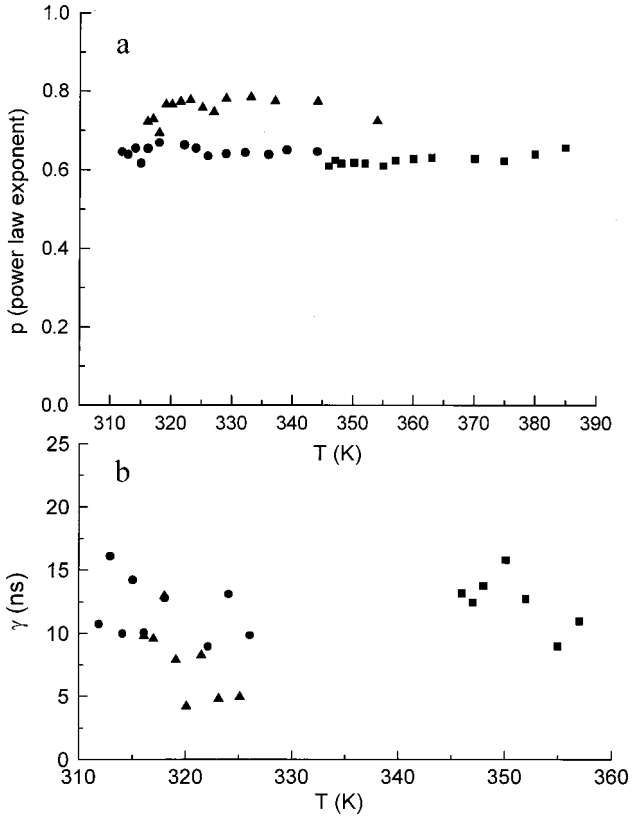

FIG. 9. (a) The power law exponents, p, obtained from fits of the data to Eq. (2), as a function of temperature for 5-OCB (squares), 5-CB (circles), and 3-CHBT (triangles). The power law exponents for all three liquids are constant, within experimental uncertainty, over the full temperature ranges studied. The p values are 0.63 ± 0.01 (5-OCB), 0.65 ± 0.01 (5-CB), and 0.76 ± 0.03 (3-CHBT). (b) The intermediate exponential decay constants, γ, as a function of temperature. Within experimental error, the γ are temperature independent or weakly temperature dependent.

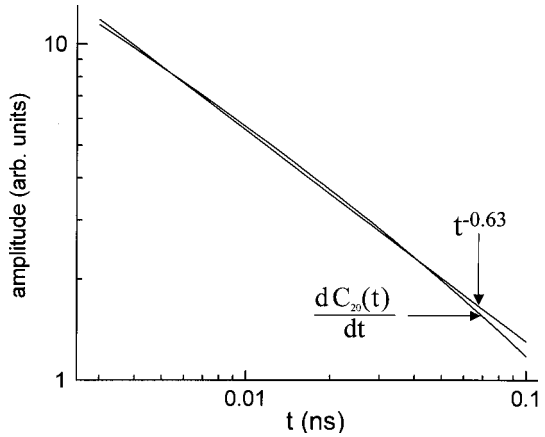

FIG. 10. The time derivative of the theoretical correlation function, $C_{20}(t)$ [Eq. (5)]. Also shown is a $t^{-0.63}$ power law (5-OCB). At short time, the derivative of the theoretical correlation function decays essentially as a power law. By the proper choice of the parameter, a, the decay can be made to match the short time portion of the experimental data.

at relatively short times, the polarizability–polarizability time correlation function will have a weak time dependence (see below).

The details of the analysis leading to Eq. (5) (Ref. 23) suggests that the weak time dependence on time scales that are short compared to τ_{LdG} is a direct consequence of pseudonematic domain formation as the *NI* transition is approached from the isotropic phase. The pseudonematic domains give rise to slow, local orientational density fluctuations, which in turn affect the orientational friction because the torque–torque correlation function is coupled to these fluctuations. The influence of the domains on the local orientational density fluctuations is reflected in a strong frequency dependence of the rotational friction in the low frequency range. The strong frequency dependence of friction acts in the opposite manner to the usual decay from the short-range interactions, nearly canceling it. At long times, ($t\geqslant\tau_{\mathrm{LdG}}$) this frequency dependence dies down, and the LdG theory should be recovered. One, therefore, expects a nonexponential crossover region where nonexponential decay at short times will go over to the long time scale exponential decay. This crossover region is akin to the von Schweidler region[33,34] of the dynamics observed in supercooled liquids.[27,35] It arises for essentially the same reason, that is, the stretching of relaxation at intermediate times. As the relaxation proceeds after the initial fast decay, the friction due to intradomain correlations increases rapidly. This increase leads to the slow power-law decay.

The correlation function given in Eq. (5) has a very different form from the experimentally derived empirical correlation function given in Eq. (4). The function given in Eq. (4) spans the full time range from ps to $t>\tau_{\mathrm{LdG}}$. Its derivative, Eq. (2), describes the data well (see Fig. 2). Figure 10 shows a comparison between the derivative of the theoretical correlation function [Eq. (5)] and a power law with exponent -0.63 that begins the decay of the 5-OCB signal. The value of parameter $a=1.25$ in Eq. (5) was chosen to most closely match the short time power law decay. As can be seen in Fig. 10, the derivative of the theoretical correlation function is almost a power law at short time, from 3 ps to $\sim$50 ps. After that, it begins to tail off. Figure 10 is not intended to be a fit to the data. It is only used to demonstrate that the correlation function given in Eq. (5) can have the appropriate short time behavior. The decay of the 5-CB data begins with a power law with exponent -0.65. The a value that produces the same type of agreement as displayed in Fig. 10 is virtually the same as found for 5-OCB because the power law exponents are so similar. For 5-CB, $a=1.3$. The decay of the 3-CHBT data begins with a power law with exponent -0.76, which is substantially different from the other two nematogens. The a value that produces the same type of agreement as displayed in Fig. 10 is $a=3$.

While all three liquid crystals display temperature independent power law decays at short times, the values of the power law exponents vary. The power law exponents are -0.63, -0.65, and -0.76 for 5-OCB, 5-CB, and 3-CHBT, respectively. Because the short time decay depends on the collective dynamics of the nematogens, it is reasonable to assume that the details of the decay depend on the details of the nematogens' molecular interactions and structures. Table I gives the approximate lengths, widths, and aspect ratios for the three nematogens. The lengths and widths were obtained from a structural optimization using a 3D CHARMM force field. While the calculations should be considered approxi-

TABLE I. Size parameters of the nematogens.

	Length	Width	Aspect ratio	Power law exponent, p
5-OCB	17.9 Å	4.5 Å	3.98	−0.63
5-CB	16.7 Å	4.5 Å	3.71	−0.65
3-CHBT	15.3 Å	4.7 Å	3.26	−0.76

mate, particularly in the absence of intermolecular interactions that exist in the liquid, the results should be of sufficient accuracy to examine qualitatively.

Looking at Table I, there appears to be a relationship between the aspect ratio and the power law exponent. 5-OCB has the largest aspect ratio and the smallest power law exponent. 5-CB has a somewhat smaller aspect ratio and a somewhat larger power law exponent. 3-CHBT has a substantially smaller aspect ratio and a substantially larger power law exponent. The widths of the three nematogens are almost the same. The aspect ratio is predominately determined by the length of the nematogens. A larger power law exponent corresponds to a faster short time decay. Table I suggests that as the length and aspect ratio decreases, the rate of collective orientational relaxation increases.

As the length of a nematogen increases, it leads to a greater orientational correlations within the pseudonematic domains. Computer simulation studies on model nematogens (like prolate ellipsoids) show that if the aspect ratio is less than approximately 2.5, then the nematic phase itself becomes unstable.[22] The value of the order parameter in the nematic phase is a function of the aspect ratio, especially for the small aspect ratios being considered here. It is indeed remarkable that this rather subtle effect appears to have been captured in the power law decay exponent.

IV. CONCLUDING REMARKS

The temperature dependent data for the three liquid crystals are fundamentally the same (see Figs. 3, 4, and 5). The full time range of the data, from a few ps to hundreds of ns, is described well by the function given in Eq. (2). The short time decay is a power law (see Fig. 8). The long time decay is an exponential (see inset Fig. 6). Between the long time LdG exponential decay and the short time power law decay is an intermediate time scale exponential decay. In all three liquid crystals, the substantial temperature dependence of the long time exponential is well described by the LdG theory (see Figs. 6 and 7). In contrast to the long time portion of the data, the intermediate time scale exponential decay is either temperature independent, or, at most, very mildly temperature dependent [see Fig. 9(b)]. As can been seen in Fig. 9(a), the power law exponents, which determine the short time portions of the decays, are temperature independent over a wide range of temperatures.

The initial theoretical treatment of the short time dynamics, which was presented previously,[23] describes the short time behavior in terms of the collective motions of the nematogens that are locally ordered in pseudonematic domains. On time scales that are short compared to τ_{LdG} and a distance scale that is short compared to the psuedonematic domain correlation length ξ [see Eq. (1)], the dynamics are determined by the nature of the collective motions of the locally nematically ordered structures. The theoretical treatment[23] also suggested a rationale for the lack of temperature dependence at short times, but a definite explanation is not yet in hand. Extensions of the theoretical treatment that led to Eq. (5) are in progress. These include detailed molecular dynamics simulations, which should provide a more detailed view of the nature of the collective dynamics that lead to the orientational relaxation of nematogens on short time scales. Another unexplored issue is the aspect ratio dependence of the slow decay. An interesting and unanswered question is the nature of the dynamics in the nematic phase on fast time scales. As the phase transition is approached from the isotropic phase, the pseudonematic domain correlation length goes to infinity, as does τ_{LdG}. Because the dynamics at times short compared to τ_{LdG} are temperature independent and are determined by the local nematic structure that exists on short distance scales, it is possible that there will be no discontinuity in the short time dynamics as the system passes from the isotropic phase to the nematic phase.

ACKNOWLEDGMENTS

One of the authors (B.B.) would like to thank the Theoretical Chemistry Institute of the University of Texas at Austin for support of his stay in the United States, which contributed to this work. This research was supported by the National Science Foundation (DMR-0088942).

[1] P. G. de Gennes, Phys. Lett. **30A**, 454 (1969).
[2] P. G. de Gennes, *The Physics of Liquid Crystals* (Clarendon, Oxford, 1974).
[3] G. K. L. Wong and Y. R. Shen, Phys. Rev. Lett. **30**, 895 (1973).
[4] E. G. Hanson, Y. R. Shen, and G. K. L. Wong, Phys. Rev. A **14**, 1281 (1976).
[5] T. D. Gierke and W. H. Flygare, J. Chem. Phys. **61**, 22331 (1974).
[6] T. W. Stinson III and J. D. Litster, Phys. Rev. Lett. **25**, 503 (1970).
[7] J. D. Litster and T. W. Stinson III, J. Appl. Phys. **41**, 996 (1970).
[8] J. C. Fillippini and Y. Poggi, Phys. Lett. **65A**, 30 (1978).
[9] W. H. de Jeu, in *Solid State Physics*, edited by L. Liebert (Academic, New York, 1978), p. 109.
[10] H. Kresse, in *Advances in Liquid Crystals*, edited by G. H. Brown (Academic, New York, 1983), Vol. 6, p. 109.
[11] J. J. Stankus, R. Torre, C. D. Marshall, S. R. Greenfield, A. Sengupta, A. Tokmakoff, and M. D. Fayer, Chem. Phys. Lett. **194**, 213 (1992).
[12] J. J. Stankus, R. Torre, and M. D. Fayer, J. Phys. Chem. **97**, 9478 (1993).
[13] F. W. Deeg, S. R. Greenfield, J. J. Stankus, V. J. Newell, and M. D. Fayer, J. Chem. Phys. **93**, 3503 (1990).
[14] R. Torre and S. Californo, J. Chim. Phys. Phys.-Chim. Biol. **93**, 1843 (1996).
[15] R. Torre, F. Tempestini, P. Bartolini, and R. Righini, Philos. Mag. B **77**, 645 (1998).
[16] R. S. Miller and R. A. MacPhail, Chem. Phys. Lett. **241**, 121 (1995).
[17] Y. X. Yan, L. G. Cheng, and K. A. Nelson, Adv. Infrared Raman Spectrosc. **16**, 299 (1987).
[18] Y. X. Yan and K. A. Nelson, J. Chem. Phys. **87**, 6240 (1987).
[19] Y. X. Yan and K. A. Nelson, J. Chem. Phys. **87**, 6257 (1987).
[20] F. W. Deeg, J. J. Stankus, S. R. Greenfield, V. J. Newell, and M. D. Fayer, J. Chem. Phys. **90**, 6893 (1989).
[21] A. Sengupta and M. D. Fayer, J. Chem. Phys. **102**, 4193 (1995).
[22] S. Ravichandran, A. Perera, M. Moreau, and B. Bagchi, J. Chem. Phys. **109**, 7349 (1998).
[23] S. D. Gottke, D. D. Brace, H. Cang, B. Bagchi, and M. D. Fayer, J. Chem. Phys. **116**, 360 (2002).

[24] D. McMorrow, W. T. Lotshaw, and G. A. Kenney-Wallace, IEEE J. Quantum Electron. **24**, 443 (1988).
[25] D. McMorrow and W. T. Lotshaw, J. Phys. Chem. **95**, 10395 (1991).
[26] Y. Kai, S. Kinoshita, M. Yamaguchi, and T. Yagi, J. Mol. Liq. **65-6**, 413 (1995).
[27] S. D. Gottke, D. D. Brace, G. Hinze, and M. D. Fayer, J. Phys. Chem. B **105**, 238 (2001).
[28] M. Abramowitz and I. A. Stegun, *Handbook of Mathematical Functions* (Dover, New York, 1970).
[29] G. R. Fleming, *Chemical Applications of Ultrafast Spectroscopy* (Oxford, New York, 1986).
[30] B. Bagchi and A. Chandra, Adv. Chem. Phys. **80**, 1 (1991).
[31] P. Boon and S. Yip, *Molecular Hydrodynamics* (McGraw–Hill, New York, 1980).
[32] B. Bagchi and R. Biswas, Adv. Chem. Phys. **109**, 207 (1999).
[33] W. Götze and L. Sjögren, Rep. Prog. Phys. **55**, 241 (1992).
[34] W. Götze, J. Phys.: Condens. Matter **11**, A1 (1999).
[35] G. Hinze, D. D. Brace, S. D. Gottke, and M. D. Fayer, J. Chem. Phys. **113**, 3723 (2000).